Analysis of the microstructure of silicon quantum dot superlattice embedded microcrystalline silicon carbide for solar cell application

Partha Chaudhuri, Arindam Kole and Golam Haider

Indian Association for the Cultivation of Science, Kolkata, West Bengal, 700032, India

***Abstract* — We have recently demonstrated [1] p-i-n structure diodes with the intrinsic (i) layers comprising of periodic depositions of silicon quantum dot embedded microcrystalline silicon carbide and silicon rich microcrystalline silicon carbide layers by rf (13.56 MHz) plasma enhanced chemical vapour deposition method. The rf power was toggled between 80 mW/cm^3 and 40 mW/cm^3 in successive layers. The high power layer (HPL) contains silicon nanocrystallites which forms a layer of silicon quantum dots in HPL having thickness within the limit of silicon excitonic Bohr radius (~5nm). The low power layer (LPL) forms a silicon rich microcrystalline silicon carbide layer when thickness is large but becomes nearly amorphous at low thicknesses. By optimizing the layer thicknesses of HPL and LPL the interaction between the quantum dots in alternate HPL layers gave rise to the formation of an intermediate band gap resulting in good photovoltaic properties of the diode. In this paper we report an analysis of the ellipsometric data of a series of the multilayered samples of HPL having thickness at 5 nm and LPL thickness controlled between 13 nm and 2 nm to observe the evolution of the microstructure near the formation of the intermediate band. The imaginary part of the pseudodielectric function data of the multilayered samples obtained from ellipsometry have been fitted with the help of effective medium approximation method using the respective microcrystalline silicon carbide films i.e. HPL or LPL together with the phase separated poly silicon and voids as the reference materials for modeling, we observe that the volume fraction of the nanocrystalline silicon increases while the void fraction decreases within the superlattice with the lowering of the LPL thickness from 13 nm to 2 nm. These data are consistent with the evolution of the short range order within the multilayer samples and may serve as a guideline for designing the silicon quantum dot based solar cells.**

***Index Terms* — microcrystalline silicon carbide, silicon quantum dot superlattice, photovoltaic cells.**

I. Introduction

In order to find a global solution for the large scale electricity generation directly from the sunlight extensive research is going on to find suitable materials for solar cells. Besides high efficiency for conversion of solar energy to electrical energy other necessary criteria for the choice of the materials include the high abundance, the environmental friendliness, good stability, low cost technology, short energy payback period etc. for commercial solar modules. In this respect amorphous silicon which meets several of these criteria has already entered the solar cell market but still requires further improvement of the conversion efficiency. One way to achieve this is to absorb larger portion of the solar spectrum. Multijunction solar cell with band gaps for individual junctions tuned to obtain the maximum conversion efficiency is one way to enhance the efficiency for amorphous silicon based solar cells. Over small area best conversion efficiency obtained in a structure a-Si/nc-Si/nc-Si (tandem) is 12.5% [2]-[3]. In this respect another possible device structure may be an all silicon tandem solar cell with individual junctions containing size controlled silicon quantum dots which absorb specific portions of solar spectrum more efficiently [4]. The thin periodic multilayers of silicon and/or its dielectric alloys, such as Si/SiO_2, Si/SiN, Si/SiC, SiO/SiO_2, SiC/SiN etc. with embedded silicon quantum dots can give rise to strong enhancement in the absorption / emission properties by the formation of intermediate band gaps within the wider dielectric band gap [5]-[11]. The thickness of the silicon quantum dot embedded layers determines the intermediate band gap. A good interaction between the successive silicon quantum dot layers is necessary for the formation of the intermediate band. The layers of amorphous silicon carbide [12]-[16] with embedded silicon quantum dots or the multilayer structure with alternating layers of a-SiC and silicon quantum dots [17] deposited by plasma enhanced chemical vapour deposition (PECVD) method are particularly interesting because they may be easily integrated with the present day amorphous silicon solar cell technology. We have recently reported significant improvement in the short range order and quantum confinement effect leading to the formation of the intermediate band with energy gap around 1.7 eV in a microcrystalline silicon carbide (μc-SiC:H) superlattice with embedded silicon quantum dot (SiC-QDSL) by controlling the thickness of the alternate μc-SiC:H layers each having identical band gap of 2.2 eV but differing in c-Si volume fractions and demonstrated usefulness of the SiC-QDSL structures in the solar cells [1]. In order to understand the evolution of microstructures in the vicinity of intermediate band formation we report in this paper detailed analysis of the superlattice structures by modeling the spectroscopic ellipsometry data of these samples and compared the results with their Raman analysis.

II. EXPERIMENTAL

The μc-SiC:H multilayer samples designated by #SiC-ML*x* where *x* denotes the sample number were deposited in a rf (13.56 MHz) plasma enhanced chemical vapour deposition (PECVD) system from a mixture of SiH_4 and CH_4 in 1:1 ratio diluted by 98.4 volume percent of Ar at a temperature of 200°C and pressure of 26.6 Pascal. The successive μc-SiC:H

layers were prepared by toggling the rf power level between 80 mW/cm^3 for high power layer (HPL) and 40 mW/cm^3 for the low power layer (LPL). A series of four such multilayer samples were prepared each with 30 periods of alternating layers of HPL with fixed thickness of 5 nm and LPL with thicknesses of 13 nm for #SiC-ML1, 9 nm for #SiC-ML2, 5nm for #SiC-ML3 and 2 nm for #SiC-ML4 respectively (Table I). The thicker individual layers #µc-SiC:H1 and #µc-SiC:H2 were deposited using the same deposition parameters as of HPL and LPL respectively. The #SiC-ML*x* (*x*=1 – 4) and the #µc-SiC:H*y* (*y*=1 – 2) samples were deposited on optically flat quartz substrates. Structural investigations were done by Raman spectroscopy using 514.5 nm line of Ar$^+$ ion laser for excitation and by phase modulated spectroscopic ellipsometry over the UV–visible-NIR range (0.5 – 5.5 eV).

TABLE I
THICKNESS OF THE SAMPLES

Sample No.	Thickness of HPL (nm)	Thickness of LPL (nm)	No. of cycles of HPL/LPL
#SiC-ML1	5	13	30
#SiC-ML2	5	9	30
#SiC-ML3	5	5	30
#SiC-ML4	5	2	30
#µc-SiC:H1	350	-	Single layer
#µc-SiC:H2	-	350	Single layer

III. RESULTS AND DISCUSSIONS

Spectroscopic ellipsometry is an optical non-destructive method for structural analysis of the thin films. From the ellipsometric angles Ψ and Δ, the complex pseudo dielectric function ε may be calculated from the relation,

$$\langle \varepsilon \rangle = \sin^2 \Phi \left[1 + \left(\frac{1-\rho}{1+\rho} \right)^2 \tan^2 \Phi \right] \qquad (1)$$

where,

$$\rho = {r_p}/{r_s} = \tan(\Psi) \exp(i\Delta) \qquad (2)$$

r_p and r_s being the complex Fresnel reflection coefficients of light which is polarized parallel and perpendicular to the plane of incidence and Φ is the angle of incidence which is 72^0 for this study. Again writing ε as $\langle \varepsilon \rangle = \langle \varepsilon_r \rangle + i \langle \varepsilon_i \rangle$ the real and complex parts of ε, ε_r and ε_i may be calculated as a function of energy of the incident photons over the UV – visible-NIR range. By making an intelligent guess about the components of the layers the experimental values of the dielectric function of each layer may be fitted with the known dielectric function values of these components over the experimental range of wavelength using Bruggeman effective medium approximation (BEMA) [18] method as;

$$\sum_i f_i \frac{\varepsilon_i - \varepsilon_{eff}}{\varepsilon_i + 2\varepsilon_{eff}} = 0 \qquad (3)$$

where the effective imaginary pseudo dielectric function ε_{eff} of the layer may be expressed in terms of ε_i of its constituents. This way the compositions of the layers in terms of the chosen components may be obtained without actually destroying the film. This method has been very useful in depth profiling of the thin film layers containing µc-Si [19]-[21].

In Fig. 1 the scattered symbols represent the energy dependences of the experimental values of imaginary part ε_{exp} of pseudo dielectric function of the #SiC-MLx (x= 1- 4) multilayer samples. For structural analysis by BEMA method we consider #µc-SiC:H1 and #µc-SiC:H2 as well as fine grain

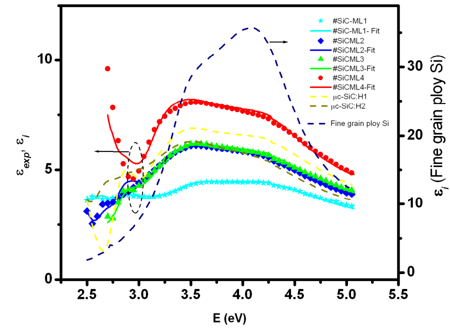

Fig. 1 Imaginary part of the pseudo dielectric function, ε_{exp} vs Energy, E (eV) of the incident photons for the multilayered samples #SiC-ML1, #SiC-ML2, #SiC-ML3 and #SiC-ML4 (scattered data) and the ε_i of the reference materials #µc-SiC:H1, #µc-SiC:H2 and p-Si (dotted curves) are shown. The Simulation curves (continuous lines) obtained using the recipe mentioned in the text are also shown.

poly silicon or p-Si and void as constituents for the layers. We have chosen #µc-SiC:H2 and void as constituents of each LPL layer while #µc-SiC:H1 and p-Si as constituents of each HPL layer. The energy distribution of the ε_i values of #µc-SiC:H1, #µc-SiC:H2 and p-Si [22] are also shown in Fig. 1. Corresponding to the best fitted (χ^2 values ranging between 0.3 and 1) curves of the experimental datasets for #SiC-ML*x* (*x* = 1 - 4) the percentage composition of the constituents in the different layers were determined.

This is shown with the help of a bar graph in Fig. 2 for the #SiC-ML4 sample. The proportions of the constituents

in the layers are represented by the length of the corresponding colour bars. From the bargraph we observe in some of the LPL layers the void is predominant while fine grain polysilicon

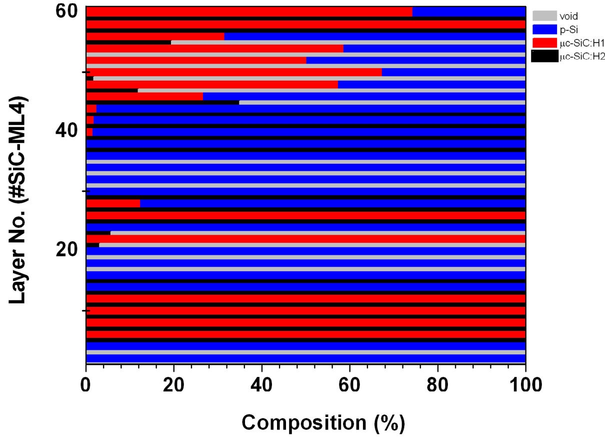

Fig. 2 Composition of the 60 number of layers of the #SiC-ML4 sample used for the simulation of the corresponding graph in Fig. 1.

dominates some of the HPL layers. The fine grain polysilicon represent the nc-Si present in the sample.

The Fig. 2 directly gives the total void fraction (f_V) and the total nanocrystalline silicon volume fraction ($C_{nc\text{-}Si}$) within #SiC-ML4. The f_V and $C_{nc\text{-}Si}$ for each of the samples #SiC-MLx (x=1-4) determined by the above method are plotted in Fig. 3. A continuous decrease of f_V from 55% to 33% and an increase in the $C_{nc\text{-}Si}$ from 22.3 % to 45.6% is

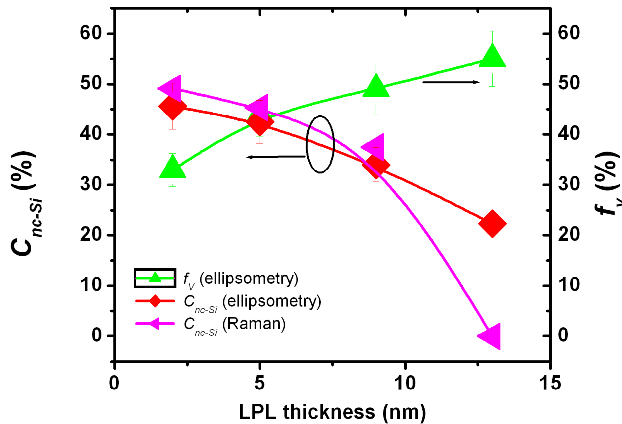

Fig. 3 Variation of the nanocrystalline silicon volume fraction ($C_{nc\text{-}Si}$) and the void fraction (f_V) with the thickness of the LPL layer. The lines are drawn as guides to the eye.

observed as the LPL thickness decreases from 13 nm to 2 nm. A constant error bar of 10% has been added to the data plots.

The nanocrystalline silicon volume fraction ($C_{nc\text{-}Si}$) calculated from the Raman analysis is also shown simultaneously in Fig. 3. The $C_{nc\text{-}Si}$ values determined from the ellipsometry and Raman analysis show similar trend with the variation of LPL thickness. There are only a few reports on the spectroscopic ellipsometry of SiC:H deposited by PECVD method [23]. We have earlier reported [1] only the void fraction obtained from ellipsometry. In the present analysis by appropriate modeling of all the layers within the #SiC-ML samples the ellipsometric data helped us to calculate both the void fraction and the nanocrystalline silicon volume fraction in the multilayer samples. It has been observed that during the a-Si:H to μc-Si:H phase transition a gradual increase of ellipsometrically determined f_V occurs with the increase in the film thickness in the mixed phase region of a-Si+μc-Si and with complete transition into μc-Si phase in case of a thicker layer f_V decreases [24]-[25]. In the mixed phase region of a-Si+μc-Si the void fraction and crystalline silicon volume fraction have been found to increase simultaneously with film thickness [20]. The studies of the #SiC-ML series using Raman spectroscopy show that the #SiC-ML*x* (*x*=2-4) samples have only nanocrystalline silicon present in them with no microcrystalline silicon contribution, while, only #SiC-ML1 has some microcrystalline silicon component but negligible nanocrystalline silicon component [1]. Hence larger LPL thickness (as in #SiC-ML1) favours μc-Si formation with more voids. Earlier we have also noted the #SiC-ML*x* layers become more compact with improvement of the short range order with the decrease of the LPL thickness keeping the HPL thickness fixed at 5 nm. Formation of an intermediate band gap within the superlattice was found to accompany this improvement of the order. In this report our observation that the $C_{nc\text{-}Si}$ increases while the f_V decreases monotonically with the decrease of the LPL thickness therefore supports earlier data and gives a new insight in to the growth of the superlattice near the intermediate band formation. Together with our earlier observations it clearly shows that the formation of the intermediate band requires more compact and ordered network of periodic array of silicon quantum dot embedded layers separated by thin dielectric layers. The material #SiC-ML*4* which has the lowest f_V and highest $C_{nc\text{-}Si}$ has been found to give significant photovoltaic properties as the intrinsic (i) layer in a p-i-n structure diode [1]. The ellipsometric analysis therefore may serve as a simple non-destructive method to check the device applicability of the #SiC-ML samples.

IV. CONCLUSIONS

The ellipsometric analysis of the series of #SiC-ML samples by means of effective medium theory using a combination of #μc-SiC:H1, #μc-SiC:H2, poly Si and void as constituent materials for each of the 60 layers have resulted in a very good simulation of the data. A clear trend of evolution of the nanocrystalline silicon volume fraction and the voids in the materials was obtained. Interestingly, it has been observed

that increase of the nanocrystalline silicon volume fraction within the #SiC-ML layers is accompanied by a decrease of the voids. This gives a simple test for the formation of the intermediate band and photovoltaic quality #SiC-ML. The work thus shows the importance of the ellipsometric analysis for the choice of the device quality #SiC-ML for solar cell application.

ACKNOWLEDGEMENT

This paper is based upon work supported in part under the US-India Partnership to Advance Clean Energy-Research (PACE-R) for the Solar Energy Research Institute for India and the United States (SERIIUS), funded jointly by the U.S. Department of Energy (Office of Science, Office of Basic Energy Sciences, and Energy Efficiency and Renewable Energy, Solar Energy Technology Program, under Subcontract DE-AC36-08GO28308 to the National Renewable Energy Laboratory, Golden, Colorado) and the Government of India, through the Department of Science and Technology under Subcontract IUSSTF/JCERDC-SERIIUS/2012 dated 22nd Nov. 2012.

REFERENCES

[1] P. Chaudhuri, A. Kole and G. Haider, "Structural characterization of superlattice of microcrystalline silicon carbide layers for photovoltaic application", Journal of Applied Physics., vol. 113, pp. 64313-64320, 2013.

[2] B. Yan, G. Yue, S. Guha., "Status of nc-Si:H solar cells at United Solar and roadmap for manufacturing a-Si:H and nc-Si:H based solar cells", Materials Research Society Symposium Proceedings, Vol. 989, Materials Research Society: Warrendale, PA, 2007, Paper #: 0989-A15-01.

[3] M. A. Green, K. Emery, Y. Hishikawa, W. Warta and E. D. Dunlop; "Solar cell efficiency tables (version 39)", Progress in Photovoltaics: Research and Applications, vol. 20, pp.12–20, 2012.

[4] X. J. Hao, E.-C. Cho, C. Flynn, Y. S. Shen, S. C. Park, G. Conibeer, and M. A. Green, "Synthesis and characterization of boron-doped Si quantum dots for all-Si quantum dot tandem solar cells", Solar Energy Materials and Solar Cells, vol. 93, pp. 273-279, 2009.

[5] L. Tsybeskov, K. D. Hirschman, S. P. Duttagupta, M. Zacharias, P. M. Fauchet, J. P. McCaffrey, and D. J. Lockwood, "Nanocrystalline-silicon superlattice produced by controlled recrystallization", Applied Physics Letters, vol. 72, pp. 43-45, 1998.

[6] L. X. Yi, J. Heitmann, R. Scholz, and M. Zacharias, "Phase separation of thin SiO layers in amorphous SiO/SiO_2 superlattices during annealing", Journal of Physics: Condensed Matter, vol. 15, pp. S2887-S2895, 2003.

[7] B. T. Sullivan, D. J. Lockwood, H. J. Labbe, and Z. H. Lu, "Photoluminescence in amorphous Si/SiO_2 superlattices fabricated by magnetron sputtering", Applied Physics Letters, vol. 69, pp. 3149-3151, 1996.

[8] Z. Wan, R. Patterson, S. Huang, M. Green and G. Conibeer, "Ultra-thin silicon nitride barrier implementation for Si nano-crystals embedded in amorphous silicon carbide matrix with hybrid superlattice structure", Europhysics Letters, vol. 95, pp. 67006-67010, 2011.

[9] A. Gencer Imer, I. Yildiz and R. Turan, "Fabrication of Si nanocrystals in an amorphous SiC matrix by magnetron sputtering", Physica, vol. E 42, pp. 2358-2363, 2003.

[10] B. Berghoff, S. Suckow, R. Rölver, B. Spangenberg, H. Kurz, A. Sologubenko, J. Mayer, "Quantum wells based on Si/SiO_x stacks for nanostructured absorbers", Solar Energy Materials and Solar Cells, vol. 94, pp. 1893-1896, 2010.

[11] D. Di, I. Perez-Wurfl, G. Conibeer, M. A. Green, "Formation and photoluminescence of Si quantum dots in SiO_2/Si_3N_4 hybrid matrix for all-Si tandem solar cells", Solar Energy Materials and Solar Cells, vol. 94, pp. 2238-2243, 2010.

[12] Eun-Chel Cho, M. A. Green, G. Conibeer, D. Song, Young-Hyun Cho,G. Scardera, S. Huang, S. Park, X. J. Hao, Y. Huang, and L.V. Dao, "Silicon Quantum Dots in a Dielectric Matrix for All-Silicon Tandem Solar Cells", Advances in Opto Electronics vol. 2007, pp. 069578-069588, 2007.

[13] Q. Cheng, E. Tam, S. Xu and K. Ostrikov, "Si quantum dots embedded in an amorphous SiC matrix: nanophase control by non-equilibrium plasma hydrogenation", Nanoscale, vol. 2, pp. 594-600, 2010.

[14] Y. Rui, S. Li, J. Xu, C. Song, X. Jiang, W. Li, K. Chen, Q. Wang and Y. Zuo, "Size-dependent electroluminescence from Si quantum dots embedded in amorphous SiC matrix", Journal of Applied Physics, vol. 110, pp. 064322-064327, 2011.

[15] A. Kole and P. Chaudhuri, "A study of the evolution of the silicon nanocrystallites in the amorphous silicon carbide under argon dilution of the source gases", Journal of Nano-Electronic Physics, vol. 3, pp. 155-161, 2011.

[16] A. Kole and P. Chaudhuri, "Nanocrystalline silicon and silicon quantum dots formation within amorphous silicon carbide by plasma enhanced chemical vapour deposition method controlling the Argon dilution of the process gases", Thin Solid Films, vol. 522, pp. 45-49, 2012.

[17] Y. Kurokawa, S. Tomita, S. Miyajima, A. Yamada, and M. Konagai, "Photoliminescence from Silicon Quantum Dots in Si Quantum Dots/Amorphous SiC Superlattice", Japanese Journal of Applied Physics vol. 46, pp. L833-L835, 2007.

[18] D. A. G. Bruggeman,"Berechnung verschiedener physikalischer Konstanten von heterogenen Substanzen", Ann. Phys. (Leipzig), vol. 24, pp. 636-679, 1935.

[19] S. Hamma and P. Roca i Cabarrocas, "In situ correlation between the optical and electrical properties of thin

intrinsic and n-type microcrystalline silicon films", Journal of Applied Physics, vol. 81, pp. 7282-7288, 1997.

[20] S. Kumar, B. drevillion and C. Godet, "In situ spectroscopic ellipsometry study of the growth of microcrystalline silicon", Journal of Applied Physics, vol. 60, pp. 1542-1544, 1986.

[21] M. Losurdo, R. Rizzoli, C. Summonte, G. Cicala, P. Cappezuto and G. Bruno, "Anatomy of μc-Si thin films by plasma enhanced chemical vapour deposition: An investigation by spectroscopic ellipsometry", Journal of Applied Physics, vol. 88, pp. 2408-2414, 2000.

[22] G. E. Jellison, Jr, M. F. Chisholm, and S. M. Gorbatkin, "Optical functions of chemical vapour deposited thin film silicon determined by spectroscopic ellipsometry", Applied Physics Letters, vol. 62, pp. 3348-3350, 1993.

[23] D. K. Basa, G. Abbate, G. Ambrosone, U. Coscia and A. Marino, "Spectroscopic ellipsometry study of hydrogenated amorphous silicon carbon alloy films deposited by plasma enhanced chemical vapor deposition", Journal of Applied Physics, vol. 107, pp. 023502-023507, 2010.

[24] R. W. Collins, A. S. Ferlauto, G. M. Ferreira, Chen Chi, J. Koh, R. J. Koval, Y. Lee, J. M. Pearce and C. R. Wronski, "Evolution of microstructure and phase in amorphous, protocrystalline, and microcrystalline silicon studied by real time spectroscopic ellipsometry", Solar Energy Material and Solar Cells, vol. 78, pp. 143-180, 2003.

[25] P. Roca I. Cabarrocas, "Plasma enhanced chemical vapour deposition of amorphous, polycrystalline and microcrystalline silicon thin films", Journal of Non-Crystalline. Solids, vol. 266-269, pp. 31-37, 2000.